Resonance Raman and Optical Spectroscopic Monitoring of Heme A Redox States in Cytochrome *c* Oxidase during Potentiometric Titrations

Paul A. Harmon,[‡,§] Richard W. Hendler,[∥] and Ira W. Levin*[,‡]

Laboratory of Chemical Physics, National Institute of Diabetes and Digestive and Kidney Diseases, and Laboratory of Cell Biology, National Heart, Lung and Blood Institute, National Institutes of Health, Bethesda, Maryland 20892

Received July 8, 1993; Revised Manuscript Received November 3, 1993[⊗]

ABSTRACT: Resonance Raman spectroscopy is used to monitor the redox state of heme *a* and heme a_3 centers in cyanide-inhibited and native cytochrome oxidase during potentiometric titrations. Specific vibrational modes are resolved for each reduced heme with 441.6-nm excitation while oxidized species show vanishingly small Raman intensities. The voltage dependencies of the Raman intensities of reduced heme *a* and reduced heme a_3 modes are quantitatively measured and used to extract heme *a* and a_3 midpoint potentials. In the cyanide-bound enzyme, in which heme a_3 remains in the oxidized state, the Raman data indicate that heme *a* centers exhibit complex Nernstian behavior with two E_m values near 350 and 260 mV. In the native enzyme, this resonance Raman–potentiometric method reveals significantly different redox behavior for the two hemes. Heme *a* centers are described by two effective E_m values near 350 and 220 mV, while heme a_3 centers have lower E_m values near 260 and 200 mV. Singular value decomposition analysis of optical spectral changes supports the Raman data. These results are in contrast to models of cytochrome oxidase redox behavior in which heme *a* and heme a_3 are thought to have essentially identical midpoint potentials.

Cytochrome *c* oxidase is the terminal electron acceptor in mitochondrial electron transport. This enzyme catalyzes the reduction of dioxygen to water using electrons derived from cytochrome *c*, while simultaneously transporting protons across the inner mitochondrial membrane. In this manner, part of the redox free energy difference between cytochrome *c* and O_2 is converted to a protonmotive force. The enzyme utilizes at least four redox-active metal centers to accomplish this task: two heme A chromophores and at least two copper centers. Since an understanding of the oxidation–reduction properties of the metal centers is crucial in formulating the specific details of the thermodynamic properties and mechanisms of action of this remarkable energy-transducing enzyme, it is not surprising that this subject has been intensely investigated for over 3 decades [for reviews, see Wikström et al. (1976, 1981), Brunori et al. (1988), Chan and Li (1990), and Hendler and Westerhoff (1992)]. Particular attention has been given to the redox potentials of the two heme A centers, *a* and a_3. However, despite numerous studies utilizing either optical absorption, electron paramagnetic resonance (EPR), or magnetic circular dichroism (MCD) spectroscopy to monitor the redox state of the hemes during oxidation–reduction titrations, there remains today significant disagreement concerning the effective midpoint potentials of heme *a* and heme a_3. In this report, we reexamine the heme A potentials of solubilized cytochrome oxidase in both the native and cyanide-inhibited enzyme, using a combined resonance Raman, optical spectroscopic–potentiometric titration method (Harmon et al., 1993).

The prevailing views of the redox characteristics of cytochrome oxidase were summarized in reviews by Wikström et al. in 1981 and by Brunori et al. in 1988. Initially, using absorption difference techniques in the 605-nm spectral region to monitor the redox state of the hemes during potentiometric titrations, the enzyme was seen to exhibit two distinct $n = 1$ titrations with E_m values near 230 and 350 mV (Wilson et al., 1972; Leigh et al., 1974). The predominant view was that heme a_3 was the high-potential center and heme *a* the low-potential center [however, see Hartzell and Beinert (1976)]. EPR (Wilson et al., 1976; Palmer et al., 1976; Wikström et al., 1981, and references cited therein) and MCD (Babcock et al., 1978; Carithers & Palmer, 1981; Kojima & Palmer, 1983) spectroscopies were subsequently used to follow the redox behavior of the heme *a* and heme a_3 centers during oxidation–reduction titrations. A consideration of all the available spectroscopies data led Wikström et al. (1981) and Brunori et al. (1988) to favor the "Neoclassical" view of cytochrome oxidase redox behavior. This view was originally put forth by Nicholls and Petersen (1974), and explained the heterogeneity of heme A redox transitions as deriving from redox interactions between the two hemes. In this model, heme *a* and heme a_3 have initially equal electron affinities, with E_m values near 350 mV. Upon the reduction of one heme, the E_m of the other heme drops by about 100 mV or more due to negative cooperativity between the binding of the first and the second electron. The two "titrations" described above were therefore viewed as deriving from an equal mixture of heme *a* and heme a_3 at each voltage. Thus, one salient feature of this model is that heme *a* and heme a_3 will always be reduced or oxidized to the same extent during redox titrations. The Neoclassical model has become a widely accepted view of cytochrome oxidase redox behavior.

Hendler et al. (1986) and Pardhasaradhi et al. (1991) reported singular value decomposition (SVD) analyses of optical absorption spectral changes of purified cytochrome oxidase during potentiometric titrations. Three distinct E_m values for the heme *A* centers in the solubilized enzyme were found at 200, 260, and 340 mV. This method had the advantage of utilizing all the spectral information in the 400–700-nm region. Carbon monoxide binding to heme a_3 was used to assign the lowest E_m component to heme a_3 and the two higher E_m titrations to heme *a*. These results argued against the Neoclassical model in that distinct heme *a* and

‡ National Institute of Diabetes and Digestive and Kidney Diseases.
§ Present address: The Liposome Co., Inc., Princeton, NJ 08540.
∥ National Heart, Lung and Blood Institute.
⊗ Abstract published in *Advance ACS Abstracts*, January 1, 1994.

heme a_3 titration behavior was found. Three similar E_m values were found by Steffens and Buse (1988), but no assignments of the components were made to specific hemes. Blair et al. (1986) also measured optical absorption spectral changes in the 400–700-nm spectral region during electrochemical titrations of cytochrome oxidase. Previously published reduced minus oxidized difference spectra for heme *a* and heme a_3, which were based on inhibitor complex studies, were used to model the observed spectral changes. Blair et al. also concluded that heme *a* and heme a_3 must exhibit different redox behaviors. Similarly, Nicholls and Wrigglesworth (1989) have proposed a redox scheme in which heme *a* and heme a_3 have different midpoint potentials.

We have coupled resonance Raman spectroscopy with potentiometric electrochemical methods in order to clarify further the redox behavior of heme *a* and heme a_3 in cytochrome oxidase. 441.6-nm excitation is used for the resonance Raman measurements, as it provides unique selectivity for reduced heme *a* and heme a_3 species. Oxidized species have small resonance Raman intensities when excited at 441.6 nm. The crucial advantage of this technique is that vibrational modes due specifically to each reduced heme are observable in the 441.6-nm-excited resonance Raman spectra of cytochrome oxidase (Ching et al., 1985; Argade et al., 1986). This allows us to monitor the relative number of reduced heme *a* and reduced heme a_3 species as functions of the solution voltage by quantitating the vibrational intensities. The Raman intensities of the reduced hemes measured as a function of voltage are then fit by simple Nernstian components to extract midpoint potentials. In the cyanide-bound enzyme, where heme a_3 is effectively locked in the oxidized state, two effective midpoint potentials near 260 and 350 mV are required to describe the heme a Raman data. In the native enzyme, our results clearly show that heme *a* and heme a_3 do not have identical redox behaviors in the 100–450-mV (SHE) region. We find that at least two effective E_m values are required to describe the redox behavior of each heme; heme *a* centers are modeled well by E_m values of 350 and 220 mV, while heme a_3 centers appear to titrate at 260 and 200 mV. SVD analyses of the optical absorption spectral changes support the Raman data. Our findings are discussed in terms of several previously proposed models describing cytochrome oxidase redox behavior.

MATERIALS AND METHODS

Cytochrome oxidase was prepared from bovine heart muscle by the method of Yoshikawa et al. (1977). These preparations consisted of 0.8 mM solutions of heme A in 0.01 M sodium phosphate buffer. Cytochrome *c* (Sigma) was used as received. The redox mediators used were 1,2-naphthoquinone (K and K Laboratories, E_m = 143 mV), diaminodurene (Fluka, E_m = 230 mV), quinhydrone (Fisher Scientific, E_m = 280 mV), and either potassium ferricyanide (J. T. Baker, E_m = 430 mV) or hydroxymethylferrocene (Strem Chemicals, E_m = 405 mV). Stock solutions of the mediators were freshly prepared for each experiment. The mediators were used at concentrations of 100–200 μM, while the enzyme concentration was ca. 4 μM. For studies of the native enzyme, the titration cell containing 1 mL of buffer (63 mM sodium phosphate/125 mM KCl, pH 7.2) and the mediators was made anaerobic by initiating an argon gas purge. The stirred solution was then brought slowly to ca. 120 mV vs SHE. Cytochrome oxidase was then added and allowed to equilibrate for at least 20 min until fully reduced. The voltage was then progressively made more positive while monitoring resonance Raman and/or optical spectroscopic changes. Equilibration at each voltage required only 10–15 min at the mediator concentrations used. Spectra could also be obtained in a subsequent re-reduction experiment. The cyanide-inhibited complex was prepared by adding a small aliquot of oxygen-saturated 10 mM KCN solution to the fully reduced enzyme under argon while holding the voltage at 120 mV. It is worthwhile noting that we find as little as 30 μM KCN will result in the complete conversion of $a^{2+}a_3^{2+}$– to $a^{2+}a_3^{3+}$–CN under these conditions. The rapid formation of the $a^{2+}a_3^{3+}$–CN complex and the high affinity for cyanide that we observe are consistent with previous reports of partially reduced "cyanide-sensitive" forms of the enzyme with high cyanide affinities and rapid cyanide binding kinetics (Jones et al., 1984; Scholes et al., 1986; Wrigglesworth et al., 1988).

In our initial studies of the native enzyme, potassium ferricyanide was used as the highest E_m mediator due to its excellent equilibration with platinum electrodes and its common usage in electrochemical studies of biological redox systems. However, we have observed that above ca. 350 mV, prolonged irradiation of 100–200 μM ferricyanide solutions by the He/Cd laser (441.6 nm, 25 mW) used for the Raman measurements can lead to the release of micromolar quantities of cyanide. This light-induced release of cyanide from ferricyanide complicated re-reduction experiments. We found that cyanide release could be kept negligible by keeping ferricyanide in its reduced form, well below its E_m, and by limiting the illumination time to only 5–10 min. Hydroxymethylferrocene, found to be an adequate alternative high-potential mediator, has been used by other investigators in studies of cytochrome oxidase (Ellis et al., 1986; Blair et al., 1986).

Voltage Control, Resonance Raman, and Optical Absorption Measurements. The titration cell is described in detail elsewhere (Harmon et al., 1993). Briefly, a 1 × 1 cm absorption cuvette was fitted with four electrodes, consisting of a measuring and a working platinum electrode, each paired with a Ag/AgCl electrode. The electrode voltages and currents, under computer control, were used to raise, lower, or hold the ambient solution potential between 100 and 450 mV in the presence of the mediators. The titration cell could be made anaerobic and could provide macroscopic mixing. A white light source was coupled to the cuvette by fiber optics. The transmitted light was collected by a similar fiber optic and delivered to a diode array detector for the absorption spectral measurements. This provided approximately 500-nm spectral coverage at a resolution of about 1 nm. The entire titration cell was positioned at the focal point of a single-stage Raman spectrograph. The 441.6-nm He/Cd laser beam was brought from underneath the cuvette and imaged onto the entrance slit of the Raman spectrograph. The Raman scattered light was detected with a PAR Model 1420 detector. Resonance Raman spectra were obtained in 5–6 min with a laser power of 25 mW. The Raman intensity of the 3400-cm^{-1} mode of water was used as an internal standard in order to quantitate the reduced heme A Raman intensity changes. Self-absorption effects were negligible due to the short path length of the incident and scattered radiation; path lengths were less than 1 mm.

Data Analysis. Plots of the Raman intensities of vibrational modes due to either reduced heme *a* or reduced heme a_3 were

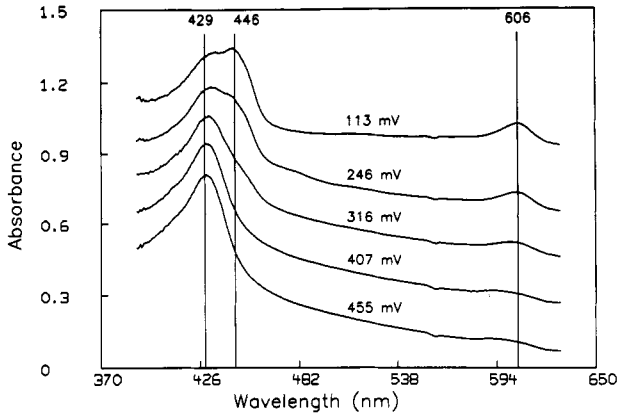

FIGURE 1: Representative absorption spectra of cyanide-bound cytochrome oxidase between 100 and 500 mV. The spectra have been vertically displaced for clarity. The lowest voltage spectrum is typical of the $a^{2+}a_3^{3+}$–CN complex, while the 455-mV spectrum is characteristic of the $a^{3+}a_3^{3+}$–CN complex with the Soret peak near 429 nm.

modeled using either a simple one- or two-component Nernstian model:

$$R_{obs} = T_1/\{1 + 10^{\wedge}[(E - E_{m1})\cdot(n_1/60)]\} + T_2/\{1 + 10^{\wedge}[(E - E_{m2})\cdot(n_2/60)]\} + d$$

where R_{obs} is the observed reduced signal, E is the solution voltage, and T_1 and T_2 are the total intensity changes for each center. E_{m1} and E_{m2}, and n_1 and n_2, respectively, are the midpoint potentials and the number of electrons characteristic of the transition from one state to the other; d represents a fitted level base line. In fitting a set of Raman data (R_{obs} versus E), a one-component model was used initially with an n value assigned to either 1 or 2. The E_m value was then extracted from the fit of the data. If the quality of the best single-component fit was clearly unacceptable, as assessed by the least-squares analysis and the signal to noise ratio of our Raman data, a two-component model was utilized. Again, n values of either 1 or 2 were assigned to each component, and the statistics of the resulting fit were examined. We stress that in this work we are more interested in whether or not the data require one or two Nernstian components rather than unambiguously establishing an n value for each titrating species. Singular value decomposition (SVD) analyses of optical absorption spectral changes were carried out as described previously (Schrager & Hendler, 1986; Hendler et al., 1986.)

RESULTS

Cyanide-Bound, Mixed-Valence Form of Cytochrome Oxidase. Figures 1–4 show absorption spectral changes and quantitative resonance Raman measurements for the potentiometric oxidation of the cyanide-bound, mixed-valence complex of cytochrome oxidase. Figure 1 shows five representative absorption spectra obtained between 113 and 455 mV. The 113-mV spectrum is characteristic of the mixed-valence complex $a^{2+}a_3^{3+}$–CN, with Soret peaks at 429 nm (a_3^{3+}–CN) and 446 nm (a^{2+}), and a peak in the visible spectral region at 606 nm, which is characteristic of reduced heme a. We have found that the oxidized, CN-bound heme a_3 center becomes reduced only at voltages of ~–200 and –300 mV. The higher voltage spectra in Figure 1 therefore reflect progressive oxidation of heme a centers with the simultaneous disappearance of both the Soret band at 446 nm and the α band at 606 nm. Figure 2 displays representative resonance Raman difference spectra in the 200–900-cm^{-1} region. All

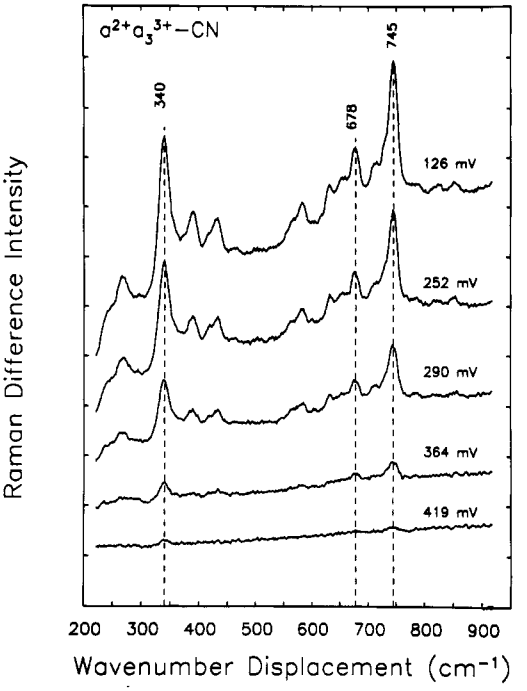

FIGURE 2: 441.6-nm-excited resonance Raman reduced minus oxidized difference spectra derived from an oxidative titration of $a^{2+}a_3^{3+}$–CN. The diminishment of all the reduced heme a vibrational mode intensities reflects the progressive oxidation of heme a centers at more positive potentials. Oxidized species have negligible Raman intensities with laser excitation at 441.6 nm.

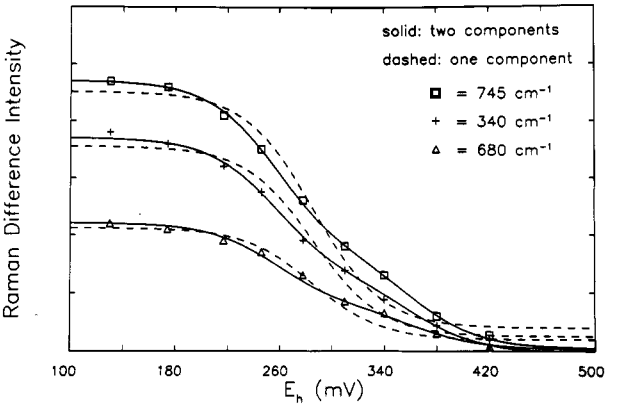

FIGURE 3: Plot of the Raman difference intensities of the 340-, 745-, and 680-cm^{-1} bands over the 100–500-mV voltage region. The dashed curves show the best single-component fits to the Raman data and clearly demonstrate systematic deviations from the observed data. The solid curve, which describes the data quite well, requires two Nernstian components (E_m = 260 mV, E_m = 365 mV) to model the heme a redox behavior.

spectra have been normalized to the 3400-cm^{-1} water mode Raman intensity. In deriving these difference spectra, the most oxidized spectrum (455 mV) was subtracted from the spectra determined at 126, 252, 290, 364, and 419 mV which were acquired during an oxidative titration. The 455-mV Raman spectrum has very weak features, on the order of 5% of that observed at 126 mV, confirming that both oxidized heme a and heme a_3^{3+}–CN centers have very small 441.6-nm-excited resonance Raman intensities. The spectral features at lower voltages shown in Figure 2 are identical to previously reported 441.6-nm resonance Raman spectra of the $a^{2+}a_3^{3+}$–CN complex (Ching et al., 1985; Ogura et al., 1985). No sign of the characteristic reduced heme a_3 modes at 213 or 365 cm^{-1} was observed after cyanide addition, which confirmed the complete formation of the cyanide-bound mixed-valence

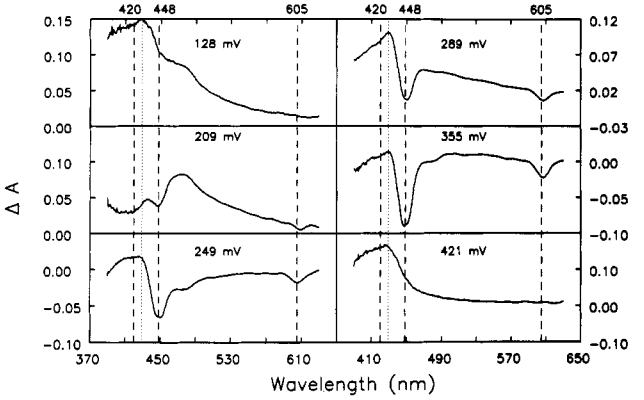

FIGURE 4: SVD analysis of the optical absorption spectral changes occurring between 370 and 630 nm during the potentiometric oxidation of $a^{2+}a_3^{3+}$–CN. The six reconstructed spectra and their relative magnitudes are displayed as oxidized minus reduced difference spectra and give the extracted E_m values (mV) of each component. The titrating components found at 128, 209, and 421 mV are those expected from 1,2-naphthoquinone, diaminodurene, and ferricyanide, respectively. The remaining heme a spectral changes are modeled as two closely spaced $n = 2$ components, with E_m values near 250 and 290 mV, and a larger magnitude $n = 1$ component, with an E_m value near 355 mV. See text for details.

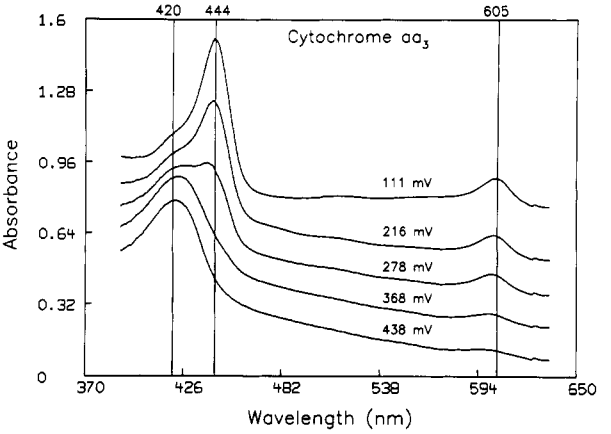

FIGURE 5: Optical absorption spectra of solubilized cytochrome oxidase obtained during potentiometric titrations. The voltage for which each spectrum was acquired is indicated. The mediators used were 1,2-naphthoquinone, diaminodurene, quinhydrone, and hydroxymethylferrocene. The 111-mV spectrum is typical of the fully reduced enzyme with a Soret maximum near 445 nm. The progressive diminishing of the 444-nm absorption feature at higher voltages should be noted as reflecting oxidation of the heme centers. The 438-mV spectrum is very similar to that of the resting enzyme except for a small contribution from oxidized 1,2-naphthoquinone.

complex. The diminishing intensities of the Raman difference spectra in Figure 2 reflect decreases in the number of reduced heme *a* centers as the solution voltage is raised.

Figure 3 shows the individual plots of the reduced minus oxidized difference Raman spectral peak intensities for the 340-, 678-, and 745-cm^{-1} modes for a complete set of Raman spectral measurements from 126 to 455 mV. The 340-cm^{-1} peak intensity was measured over a linear base line between 300 and 500 cm^{-1}, while the 678- and 745-cm^{-1} peak intensities were measured above a linear base line between 500 and 880 cm^{-1}. The 340-cm^{-1} mode intensities have been scaled by ~20% to provide clearer presentation of the data. The raw data are shown as points and simultaneous best fits by lines. Use of a model with a single $n = 1$ component produced the fits represented by dashed lines and a fitted E_m value of 285 mV. It is clear that a one-component model does not account for the data. The solid lines in the figure are derived from a simultaneous fitting of all of the Raman data to two $n = 1$ Nernstian components. The fitted E_m values were 260 and 365 mV. A two-component model thus provides a much better fit of the resonance Raman data than does the one-component model.

Singular value decomposition (SVD) analysis of full sets of optical spectra (390–630 nm) obtained under the conditions of the Raman experiments also required multiple components in order to describe the spectral changes adequately. SVD analysis required six Nernstian components to describe the heme a spectral changes and to extract the known ferricyanide, diaminodurene, and 1,2-naphthoquinone spectral responses. Reconstructed reduced minus oxidized optical spectra of each of the SVD derived components are shown in Figure 4. The 128-, 209-, and 421-mV species are similar to the known spectral characteristics of 1,2-naphthoquinone, diaminodurene, and ferricyanide and have the correct E_m values to within 10 mV. The remaining heme *a* components at 249 mV ($n = 2$), 289 mV ($n = 2$), and 355 mV ($n = 1$) are spectroscopically similar and are typical of oxidized minus reduced heme a difference spectra with 444/606-nm difference peak ratios of between 3 and 4 (Vanneste & Vanneste, 1965; Blair et al., 1983; Nicholls & Wrigglesworth, 1988). The SVD reconstructions in Figure 4 indicate that adequate modeling of the Soret and visible spectral changes requires at least two effective heme *a* E_m values, one located near 260 mV and the other at a substantially higher voltage near 350 mV.

Native Cytochrome Oxidase. Figure 5 shows representative optical absorption spectral changes monitored during a potentiometric oxidation of native cytochrome oxidase from about 110 to 450 mV. The spectra have been displaced on the absorbance axis to provide clearer presentation of the data. The 111-mV spectrum is typical of the completely reduced enzyme with a Soret peak near 444 nm and a pronounced visible region absorption band near 605 nm. As the voltage is raised, the Soret peak at 444 nm, as well as the 605-nm feature, diminishes with a concomitant increase in absorbance in the 420-nm spectral region. The highest voltage spectrum in Figure 5 (438 mV) has a minor, steadily rising absorbance contribution from 550 to 700 nm by oxidized 1,2-naphthoquinone. The Soret peak position of 422 ± 1 nm for the 438-mV spectrum is within 1 or 2 nm of that we measure when the enzyme is dispersed directly into oxygen-saturated buffer (Soret peak = 420 ± 1 nm).

Figure 6 displays low-frequency 441.6-nm-excited resonance Raman spectra obtained during a similar potentiometric oxidation of cytochrome oxidase between 120 and 300 mV. The 122-mV spectrum is consistent with previously reported resonance Raman spectra of the dithionite-reduced enzyme. All vibrational features are due to either reduced heme *a* or reduced heme a_3. The vibrational assignments given in Figures 6 and 7 are derived from previous inhibitor complex studies (Ching et al., 1985; Ogura et al., 1985; Argade et al., 1986) as well as our own results and will be discussed in greater detail below. Excitation at 441.6 nm is uniquely sensitive to reduced heme A species due to the large resonance Raman effect; as either chromophore becomes oxidized, the Raman intensities decrease dramatically as the Soret absorption peaks shift to shorter wavelengths. The four resonance Raman spectra in Figure 6 show clearly that heme A centers are significantly oxidized at 295 mV. Furthermore, there are changes in the relative peak intensities between the 122- and 295-mV spectra. This demonstrates that regardless of specific band assignments, hemes *a* and a_3 are being oxidized at different voltages. The reduced heme a_3 band at 210 cm^{-1}

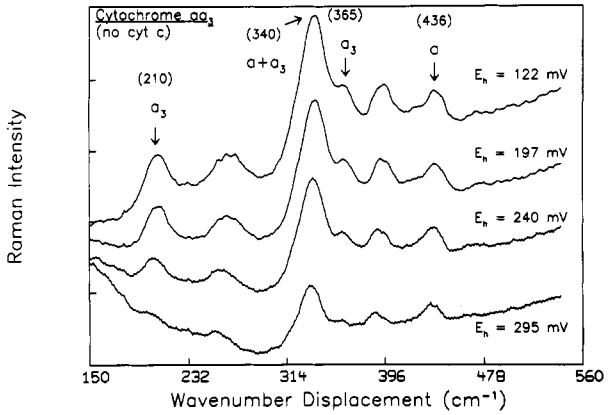

FIGURE 6: Low-frequency resonance Raman spectra, excited at 441.6 nm, of cytochrome oxidase obtained during a potentiometric oxidation between 120 and 320 mV. Potassium ferricyanide, added to the system anaerobically at 280 mV, was used as the highest potential mediator. The relative intensities of vibrational modes due to either reduced heme *a* or heme a_3 clearly change in this voltage region. A dramatic decrease in the intensity of the 210-cm^{-1}, 5-coordinate iron–histidine stretching mode is apparent.

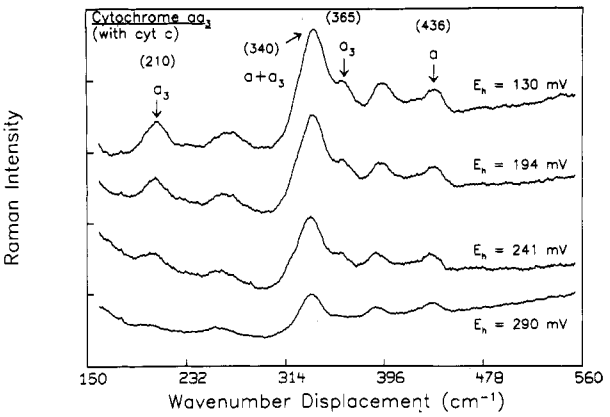

FIGURE 7: Low-frequency resonance Raman spectra as described in Figure 2, but with the addition of 0.5 equiv of cytochrome *c* as an additional mediator. The same voltage dependence of the reduced heme *a* and heme a_3 Raman intensities occurs; that is, the modes associated with heme a_3 lose intensity more rapidly as the voltage is raised.

and the shoulder at 365 cm^{-1} clearly diminish in intensity more rapidly compared to the 436-cm^{-1} reduced heme *a* mode as the voltage is raised. This demonstrates that heme a_3 centers have a lower E_m than heme *a* centers. Indeed, the 295-mV spectrum in Figure 2 is quite similar to that expected for reduced heme *a* alone (spectrum B, Figure 8).

Figure 7 shows data for an identical oxidative experiment in which approximately 2 μM cytochrome *c* was added as an additional mediator. The same voltage dependence of the vibrational spectrum as seen Figure 2 is evident; the intensities of the modes associated with reduced heme a_3 diminish more rapidly as the voltage is raised.

Because of the importance of the assignment of low-frequency modes to either heme *a* or heme a_3 to our conclusions, we show in Figure 8 the results that we have obtained concerning the isolation of the heme a^{2+} and heme a_3^{2+} spectral contributions. Similar work using both cyanide and carbon monoxide as ligands to deconvolve the 441.6-nm resonance Raman spectra of the heme a^{2+} and a_3^{2+} centers has been reported by Ching et al. (1985) and Argade et al. (1986). Our results agree, but our procedure requires no arbitrary normalization factors to generate the resonance Raman difference spectrum of "pure" heme a_3^{2+}. Spectrum A in Figure 8 shows

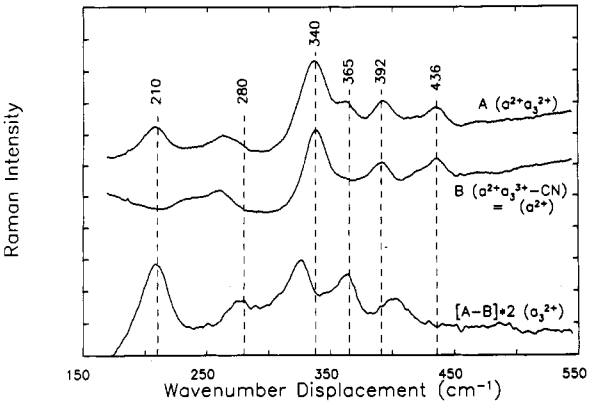

FIGURE 8: Deconvolution of the heme a^{2+} or heme a_3^{2+} low-frequency Raman signals. Spectrum A is that of the enzyme at 120 mV. Vibrational modes from both reduced hemes contribute to the spectrum. Spectrum B arises from adding a small amount of oxygen-saturated cyanide solution while maintaining the voltage at 120 mV, which results in forming the $a^{2+}a_3^{3+}$–CN species. Spectrum B originates solely from heme a^{2+}. The lower spectrum is a direct difference spectrum, A – B, which gives the low-frequency spectrum of heme a_3^{2+} with dominant features at 210, 327, and 365 cm^{-1}.

the enzyme equilibrated with the mediators under argon at 120 mV. The spectrum is characteristic of the completely reduced enzyme, as discussed previously with vibrational features due to both reduced hemes. Spectrum B was obtained after the introduction of a small aliquot of oxygen-saturated cyanide solution while holding the voltage at 120 mV; it appears identical to previously reported spectra of the $a^{2+}a_3^{3+}$–CN complex (Ching et al., 1986). The formation of $a^{2+}a_3^{3+}$–CN from $a^{2+}a_3^{2+}$ plus CN and O_2 that we observe here is consistent with the scheme recently proposed by Wrigglesworth et al. (1988) concerning CN binding to the partially reduced form of the enzyme in the presence of O_2 and reductant. Spectrum B is strongly dominated by reduced heme a modes due to the blue shift of the a_3^{2+} Soret maximum to about 429 nm upon oxidation and cyanide complexation. This blue shift leads to a much smaller 441.6-nm-excited resonance Raman effect. At 120 mV, the a_3^{3+}–CN center is not reduced; thus, the difference spectrum A – B should give the Raman spectrum of a_3^{2+}. The difference spectrum, shown as the lower spectrum in Figure 8, clearly yields features due to a_3^{2+} at 210, 279, 327, 365, and 410 cm^{-1}. The mode at 436 cm^{-1} is therefore dominated by heme *a*.

Figure 9 shows high-frequency (1200–1800 cm^{-1}) 441.6-nm-excited resonance Raman data analogous to the low-frequency data shown in Figures 6–8. Figure 9A displays the resolved high-frequency spectra of heme a^{2+} and heme a_3^{2+}, obtained as in Figure 8. The top spectrum in Figure 9A is of the fully reduced enzyme at 120 mV. The center spectrum is the same sample after conversion to the $a^{2+}a_3^{3+}$–CN complex while holding the voltage at 120 mV. This spectrum derives almost entirely from a^{2+} and is characterized by similar intensities in the 1355-, 1570-, and 1615-cm^{-1} regions as well as the complete lack of the 1664-cm^{-1} formyl mode. The lowest spectrum in Figure 9A is the direct difference spectrum, $a^{2+}a_3^{2+}$ minus $a^{2+}a_3^{3+}$–CN, giving the spectrum expected for a_3^{2+}. The a_3^{2+} spectrum is again quite different from that of heme a^{2+}. For heme a_3^{2+}, the 1355-cm^{-1} intensity is approximately 2.5 times more intense than the 1570-cm^{-1} region, while there is essentially no intensity in the 1615-cm^{-1} region. The 1664-cm^{-1} formyl mode is strong and is dervied solely from heme a_3^{2+}. Identical higher frequency Raman spectral assignments were reported previously by Ching et al. (1985).

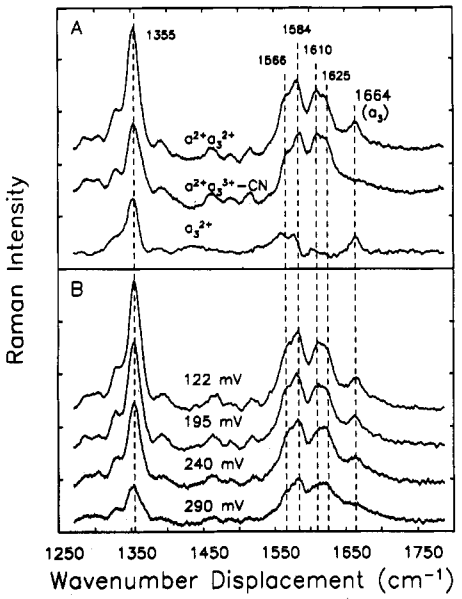

FIGURE 9: (A) Deconvolution of the heme a^{2+} or heme a_3^{3+} higher frequency Raman signals. The upper spectrum reflects the fully reduced enzyme at 120 mV ($a^{2+}a_3^{2+}$). The middle spectrum arises after the addition of an oxygen-saturated cyanide solution ($a^{2+}a_3^{3+}$–CN = a^{2+}). The lower spectrum, a direct difference spectrum, represents the high-frequency heme a_3^{2+} vibrational features. (B) High-frequency resonance Raman spectral changes occurring during the potentiometric oxidation of cytochrome oxidase. Experimental conditions are described in the caption for Figure 2. Note the disappearance of the 1664-cm^{-1} mode and the dramatic relative intensity changes between the 1355- and 1584-cm^{-1} modes.

The four representative resonance Raman spectra shown in Figure 9B were obtained during a potentiometric oxidation. It is important to note the dramatic relative intensity changes that occur as the voltage is raised. The higher voltage spectra appear increasingly similar to the spectrum of heme a^{2+} alone, showing similar intensities in the 1355-, 1570-, and 1615-cm^{-1} regions and little intensity in the 1664-cm^{-1} formyl mode (compare the 290-mV spectrum, Figure 9B, with the $a^{2+}a_3^{3+}$–CN = a^{2+} spectrum, Figure 9A). The high- and low-frequency Raman data in Figures 6–9 indicate that near 300 mV vs. SHE most heme a_3 centers are oxidized, while a significant fraction of the heme a centers remain reduced.

Figure 10 shows the quantification of the 210-cm^{-1} heme a_3^{2+} and 436-cm^{-1} heme a^{2+} resonance Raman intensity decreases observed for the potentiometric oxidations in Figure 6. The 210-cm^{-1} mode has been assigned to the iron–histidine stretching mode of 5-coordinate reduced heme a_3^{2+} (Ogura et al., 1983), while the 436-cm^{-1} mode is likely a heme a^{2+} pyrrole folding mode (Choi & Spiro, 1983). The intensity of each mode at 122 mV has been normalized to 100. The decreasing intensities for each mode reflect the conversion of a_3^{2+} and a^{2+} to oxidized species. Figure 10 clearly shows that the heme a_3 centers are more rapidly oxidized as the voltage is raised. The 295-mV spectra discussed previously originate from about 50% of the initial heme a centers remaining reduced, while only about 10% of the heme a_3 centers are reduced. The heme a_3 Raman data are fit marginally better by two $n = 2$ Nernstian components than by a single $n = 1$ component model. The solid line in Figure 10 arises from a two-component $n = 2$ model giving E_m values of 200 and 260 mV. Identical midpoint potentials are extracted from the Raman data in the presence of cytochrome c as an additional mediator.

The extent of heme a and heme a_3 reduction over a larger voltage range, between 100 and 450 mV, is shown in Figure

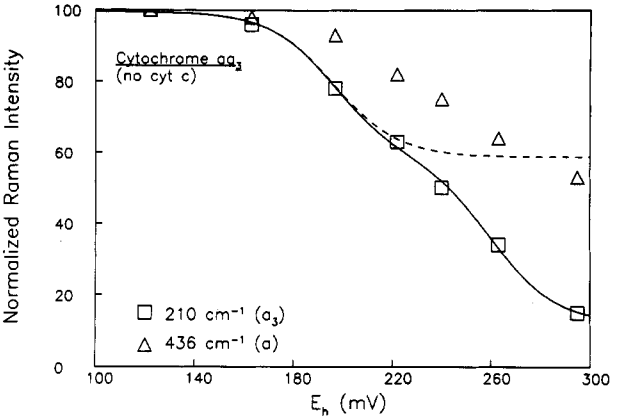

FIGURE 10: Quantification of heme a^{2+} (triangles) and heme a_3^{2+} (squares) resonance Raman intensities in the 100–300-mV region. Conditions are as described in Figure 2. The 210-cm^{-1} iron–histidine 5-coordinate heme a_3^{2+} intensities clearly diminish more rapidly than heme a^{2+} Raman intensities as the voltage is raised, which reflects the oxidation of heme a_3^{2+} centers at lower voltages. The solid curve represents a two-component Nernstian fit to the heme a_3^{2+} Raman data giving E_m values of 200 and 260 mV; the dashed curve shows the contribution from the 200-mV component.

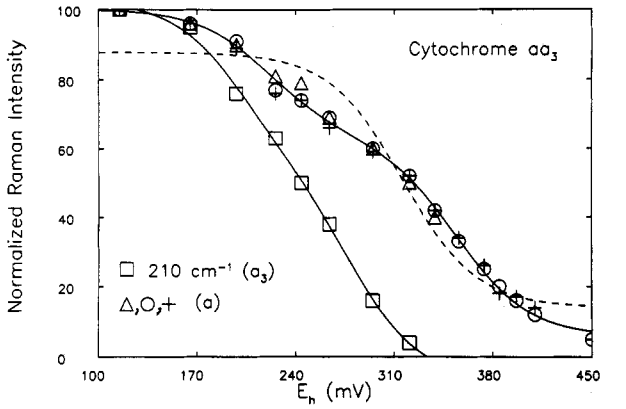

FIGURE 11: Quantification of the populations of reduced heme a (circles, crosses, and triangles) and heme a_3 (squares) between 100 and 450 mV. Hydroxymethylferrocene was used as the highest potential mediator rather than ferricyanide. The solid curve is a best fit to the 210-cm^{-1} heme a_3^{2+} data giving E_m values of 200 and 260 mV. The heme a^{2+} titration is not well described by the fit to a single Nernstian component, as shown by the dashed curve. The solid curve through the heme a^{2+} data is derived from a two-component model giving E_m values of 220 and 350 mV.

11. In these experiments, hydroxymethylferrocene was used as the highest E_m mediator rather than ferricyanide as described under Materials and Methods. The behavior of the heme a_3^{2+} 210-cm^{-1} mode (squares) and the heme a^{2+} 436-cm^{-1} mode intensities (triangles) over the 100–300-mV range is consistent with that shown in Figure 10. Quantification of the 436-cm^{-1} mode intensity above approximately 340 mV became difficult due to its weak intensity. The extent of reduction of heme a centers over the entire 100–450-mV range was monitored by measuring the intensity of the 340- and 745-cm^{-1} modes and by subtracting the amount of intensity from overlapping heme a_3^{2+} contributions. The contribution of heme a_3^{2+} at 340 and 745 cm^{-1} at each voltage was quantitated by measuring the degree of heme a_3^{2+} reduction through the 210-cm^{-1} mode intensity and by using the known relative contributions at 340 and 745 cm^{-1} derived from the "pure a_3^{2+}" Raman difference spectrum which was described in Figure 8. The quantification of the redox behavior of the heme a^{2+} centers which was monitored by the 340- and 745-cm^{-1} mode intensities in the above manner is shown by the

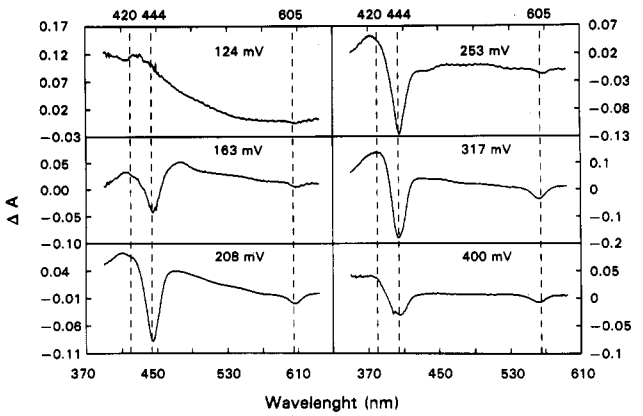

FIGURE 12: SVD analysis of optical absorption spectral changes occurring during a potentiometric oxidation between 100 and 450 mV as described in Figures 1 and 8. We show the oxidized minus reduced difference spectra of the six fitted components which most accurately modeled all the observed spectral changes. The 124-mV component originates from the mediator 1,2-naphthoquinone, while diaminodurene contributes a small positive feature near 475 nm to the 163- and 208-mV components. All remaining components originate from cytochrome oxidase. The large differences in the 444/605-nm difference peak ratios between components should be noted.

circles and crosses, respectively, in Figure 11. The 340- and 745-cm^{-1} data have also been normalized to 100 at the lowest voltage. The good agreement between the triangular, circular, and crossed data points in Figure 11 demonstrates that heme a spectral changes are being consistently monitored. A good fit to the heme a redox behavior cannot be obtained using a single $n = 1$ Nernstian component, as shown by the dashed curve in Figure 11. The heme *a* Raman data can be fit by two $n = 1$ components. This model yields fitted heme a E_m values of 350 and 220 mV (solid curve, Figure 11). The heme a_3^{2+} redox behavior is again modeled well with two $n = 2$ titrations with E_m values near 260 and 200 mV. Reduction experiments carried out after the oxidative studies led to the regeneration of the reduced heme *a* and heme a_3 spectral features with a similar voltage dependence to that presented in Figure 11 (data not shown).

Figure 12 shows reconstructed oxidized minus reduced difference spectra derived from a singular value decomposition (SVD) analysis of optical absorption spectral data obtained during a potentiometric oxidation, as described in Figure 11. For the analysis in Figure 12, absorption spectra were collected about every 13 mV between 100 and 450 mV. Within the signal to noise ratio of the measurements, the SVD data reduction analysis required six components to describe the mediator and oxidase spectral changes. The E_m value for each component is shown in Figure 12. The *n* value for all components was $n = 2$, except for the 317-mV component ($n = 1$). The 124-mV component is dominated by 1,2-naphthoquinone, and has the expected oxidized minus reduced spectral features for this mediator. The only other mediator with any significant absorbance is diaminodurene, which contributes a positive feature near 475 nm in the 163- and 208-mV component spectra in Figure 12. The remaining five components are spectral changes associated with the enzyme. While we realize the uncertainities in assigning unique molecular species to each component, it is important to point out that the components extracted by the SVD procedure and shown in Figure 12 differ significantly in their 444/605-nm oxidized minus reduced peak ratios. From Figure 12, we estimate that the 444/605-nm ratios are 8, 6, 16, 4, and 3.5 for the 163-, 208-, 253-, 317-, and 400-mV SVD derived components, respectively.

DISCUSSION

Multiple Midpoint Potentials in Cyanide-Inhibited Cytochrome Oxidase. In the cyanide-bound enzyme, heme a_3 is stabilized in an oxidized state while Cu_B may undergo oxidoreduction (Wikstrom et al., 1981; Goodman, 1984; Wrigglesworth et al., 1988). The decreasing Raman difference intensities in Figure 2 therefore originate from the progressive oxidation of reduced heme *a* centers as the solution potential is raised. The voltage dependence of the heme a^{2+} Raman intensities (Figure 3) appears to be well described by two $n = 1$ titrations near 260 and 350 mV. The SVD analysis of optical spectral changes is consistent with the Raman data in that two closely spaced $n = 2$ transitions near 270 mV and an $n = 1$ transition near 350 mV are derived which have the oxidized minus reduced spectral characteristics typical of heme a (Vanneste & Vanneste, 1965; Blair et al., 1983; Nicholls & Wrigglesworth, 1989).

These findings are probably consistent with early absorbance–potentiometric data which showed a "single" heme *a* E_m value near 300 mV with an anomalous *n* value of 0.5 (Minnaert, 1965; Hinkle & Mitchell, 1970; Wilson & Leigh, 1974; Artzatbanov et al., 1978). As pointed out by Wikström et al. (1981), this *n* value could be explained by two unresolved heme *a* titrations separated by 50–100 mV. However, Kojima and Palmer (1983) used MCD spectroscopy to monitor the redox state of heme *a* centers in the cyanide-bound enzyme and concluded that the heme *a* centers titrated as "well-behaved" $n = 1$ electron acceptors with an E_m value of 295 mV. Goodman (1984) found evidence for complex heme a titration behavior using EPR methods. An anticooperative interaction of about 50 mV between heme *a* and Cu_B was postulated. Blair et al. (1986) and Ellis et al. (1986) noted slight deviations from linearity in Nernst plots of heme *a* absorbance changes in the cyanide- and carbon monoxide-bound enzyme. The nonlinearities were modeled using "interactive" models simulating anticooperative effects. Anticooperativity between heme *a* and the copper centers was postulated. [However, for an alternative viewpoint concerning the ability of carbon monoxide to hold the heme a_3 center in the reduced state, see Hendler (1991).]

In principle, complex heme *a* redox behavior in the cyanide-bound enzyme could arise from heme *a* conformational heterogeneities or from redox cooperativity between heme *a* and another redox center (excluding heme a_3). Although our Raman and SVD data are fit well using widely separated, distinct E_m values of 260 and 350 mV, the data could have been fit just as easily by interactive models. Thus, the data presented here of itself cannot distinguish between these two different mechanisms for complex heme *a* titration behavior in the cyanide-bound enzyme. We point out, however, that the heme *a* E_m values we find in the cyanide-bound complex and in the native enzyme are consistent with a model involving anticooperative interactions that was proposed by Nicholls and Wrigglesworth (vide infra).

Heme a and Heme a_3 Have Markedly Different Redox Behaviors in the Native Enzyme. The 441.6-nm resonance Raman spectra of fully reduced cytochrome oxidase (Figures 6–9) show intense vibrational features due to heme a^{2+} and heme a^{3+}. At higher voltages, the 6-coordinate heme a^{2+} Raman intensities decrease as these centers are converted to 6-coordinate low-spin heme a^{3+} species, while the 5-coordinate low-spin heme a_3^{2+} modes diminish as these centers are

converted to oxidized species. (We point out that we cannot define the spin or coordination state of the heme a_3^{3+} species formed in the 120–130-mV region from our 441.6-nm excitation Raman data.) The crucial point is that if both the heme centers had indistinguishable redox behaviors, both hemes would oxidize identically as the voltage is raised, and no changes in the relative intensities of reduced heme and *a* and a_3 modes would occur. This is not the case, as shown by the dramatic changes in relative intensities of heme a^{2+} and heme a^{3+} modes between 120 and 300 mV (Figures 6, 7, and 9). These spectral changes clearly indicate that heme *a* and heme a_3 have different midpoint potentials. Figures 10 and 11 show that the heme *a* centers are significantly more reduced than the heme a_3 centers at all voltages above about 170 mV. At 320 mV, about 40% of the heme *a* centers are reduced while essentially all the heme a_3 centers are oxidized. Near 240 mV, 50% of the heme a_3 centers are reduced, 5-coordinate, and high-spin, while 75% of the heme *a* centers are reduced. Nernstian modeling of the heme *a* Raman intensity changes shows that the data can be described by two $n = 1$ components with E_m values of 350 and 220 mV. The heme a_3 Raman data can be described approximately by a single transition with an E_m value near 240 mV and an *n* value of 1. However, the heme a_3 data are fit better by two $n = 2$ components with E_m values of 260 and 200 mV. An $n = 2$ heme a_3 component titrating near 200 mV has been recently reported (Hendler et al., 1986; Pardhasaradhi et al., 1991).

The SVD analysis of optical absorption spectral changes occurring under identical conditions (Figure 12) is remarkably consistent with the conclusions drawn from the resonance Raman–potentiometric data and argues further for the two-component heme a_3 model. The 444/605-nm absorption difference peak ratios of each modeled component in Figure 12 can be used as a gauge to identify the likely heme *a* or heme a_3 character of the component. The 444/605-nm heme *a* oxidized minus reduced peak ratio has been found to be approximately 3–4, while for heme a_3 this ratio is much larger, about 15–20 (Vanneste & Vanneste, 1965; Blair et al., 1983; Nicholls & Wrigglesworth, 1989). The 317- and 400-mV components in Figure 12 have 444/605-nm oxidized minus reduced peak ratios of about 4 and 3.5, respectively. These values are characteristic of heme *a*. The Raman data in Figure 11 clearly show that heme *a* is indeed the only titrating species in the 300–450-mV region; the heme a_3 centers have already been oxidized. The SVD analysis derives an $n = 2$ component at 253 mV which has a 444/605-nm difference peak ratio of about 16 (Figure 12), clearly characteristic of heme a_3. In excellent agreement, the two-component modeling of the heme a_3 Raman data shows one of the heme a_3 components at 260 mV. The remaining SVD modeled component at 163 mV and the larger amplitude component at 208 mV have 444/605-nm peak ratios of about 7. This value appears intermediate between that expected for pure heme *a* or pure heme a_3, suggesting that the heme *a* and heme a_3 titrations are not being resolved by the SVD analysis in this voltage region. The interpretation is supported by the Raman data analysis which shows the E_m of the remaining heme a_3 component near 200 mV and the E_m of the lower heme *a* titration near 220 mV.

Recent Evidence for Differential Heme a and Heme a_3 Redox Behavior. Our results support the idea that heme *a* and heme a_3 have unique redox potentials. Other laboratories have recently reported distinguishable heme *a* and heme a_3 redox behaviors using absorption-based techniques. In a series of papers, Hendler and co-workers have used SVD analyses of optical absorption spectral changes to study the redox properties of purified cytochrome oxidase (Hendler et al., 1986; Pardhasaradhi et al., 1991). Two forms of the enzyme were examined: a membrane-stabilized form and the detergent-solubilized form examined here. SVD analysis of the detergent-solubilized enzyme showed three major components titrating at approximately 200, 260, and 340 mV. The unique ability of heme a_3 to bind CO was used to assign the components to either heme *a* or heme a_3. Upon carrying out the titration under a CO atmosphere, the SVD analysis showed the disappearance of the 200-mV component and the appearance of a new component near 330 mV with the spectral characteristics of the heme a_3^{2+}–CO complex. The other two SVD-modeled components had E_m values within 20 mV of the E_m values found in the absence of CO and were thus attributed to heme *a*. The resonance Raman–potentiometric method described here confirms the 200-mV heme a_3 E_m, but also reveals an additional heme a_3 E_m near 260 mV. We view the 260-mV component found by Hendler et al. (1986) and Pardhasaradhi et al. (1991) as originating from the overlapped 220-mV heme *a* and 260-mV heme a_3 titrations (Figure 11). We confirm the 340-mV transition as arising from heme *a*. It should be also be noted that when raising the voltage from about 100 mV to 450 mV, Hendler et al. (1986) viewed the 260- and 340-mV components derived from the SVD analysis as having contributions from the reduction of a high-potential form of heme a_3. This view originates from SVD experiments on the *membrane-stabilized* enzyme, in which the authors report that the enzyme has a Soret peak near 429 nm in the fully reduced form, as well as in the 450–750-mV region. Their interpretation of this observation is that heme a_3 is *reduced* in both cases. In the detergent-solubilized enzyme studied here, we see near 450 mV a Soret peak at 422 nm, which we interpret to be oxidized (low-spin) heme *a* and oxidized heme a_3 in a high or perhaps intermediate spin state. The fully reduced enzyme has a Soret peak near 446 nm. The features in the oxidized minus reduced SVD-derived components shown in Figure 12 are therefore interpreted as reflecting only the oxidation of heme *a* and/or heme a_3 as the voltage is raised from 120 to about 450 mV.

Blair et al. (1986) used difference spectra for reduced – oxidized heme *a* and heme a_3 to model absorption spectral changes occurring during redox titrations of solubilized cytochrome oxidase. The heme *a* and heme a_3 difference spectra were based on inhibitor complex studies (Vanneste & Vanneste, 1965; Blair et al., 1983). Their results also showed different Nernstian behavior for both heme *a* and heme a_3. A portion of the heme *a* centers appeared to titrate with an E_m value near 340 mV when all other centers were oxidized. Heme a_3 centers became reduced at voltages 60 to 80 mV lower. On the basis of their work and previously published data, the authors proposed anticooperative effects between heme *a* and Cu_A, Cu_B, and heme a_3, while heme a_3 could interact anticooperativity with heme *a* and Cu_B. Nicholls and Wrigglesworth (1989) proposed a model which incorporated some of the issues raised by Hendler et al. (1986) and the results of Blair et al. (1986), as well as some of their own observations. In their model, anticooperative effects account for all the observed complex Nernstian behaviors. The predicted E_m values for the hemes in this model are reviewed here inasmuch as they appear to be consistent with our results. In their model, when all the heme and copper sites are oxidized, heme a_3 centers have a low E_m value, while heme *a* centers have an E_m value near 330 mV. Upon reduction of Cu_B, the heme a_3 E_m is raised to about 280 mV. The heme a_3 E_m will be lowered to about 230 mV if heme *a* becomes reduced in

addition to Cu_B. Similarly, from the completely oxidized state, the heme *a* E_m will lower from 330 to 260 mV if Cu_B becomes reduced first and will even lower further to 210 mV if heme a_3 also becomes reduced. Thus, in the cyanide-inhibited enzyme, this model predicts heme *a* E_m values of about 330 and 260 mV since cyanide binding does not prevent Cu_B reduction (Wikstrom et al., 1981; Goodman et al., 1984; Wrigglesworth et al., 1988). We find heme *a* E_m values of 350 and about 260 mV in the cyanide-inhibited enzyme. In the native enzyme, we observe a further lowering of the heme *a* midpoint potential, such that effective E_m values of 350 and 220 mV best describe the data. This is consistent with the postulated lowering of the heme *a* E_m to 230 mV from heme *a*–heme a_3 anticooperativity. Lastly, in the native enzyme, we observe heme a_3 E_m values of 260 and 200 mV, within about 20 mV of the 280- and 230-mV heme a_3 E_m values predicted by the Nicholls and Wrigglesworth model. We stress that our data alone do not explicitly demonstrate that the complex Nernstian behavior of the heme centers is derived from anticooperative effects, but rather are consistent with a large body of evidence which indicates that such interactions exist.

In conclusion, we have coupled resonance Raman spectroscopy with potentiometric methods to examine the redox behavior of heme *a* and heme a_3 in solubilized cytochrome oxidase. Our results show that heme *a* and heme a_3 have unique redox behaviors. In the native enzyme, heme *a* centers exhibit effective E_m values of 350 and 220 mV, while heme a_3 centers have lower E_m values of 260 and 200 mV. These findings are consistent with recent reports of differential heme *a* and heme a_3 redox behavior (Hendler et al., 1986; Blair et al., 1986). The E_m values for heme *a* and heme a_3 that we determine here are similar to those proposed in a recent model by Nicholls and Wrigglesworth in which anticooperative interactions between the heme and copper centers lead to a complex, but distinguishable Nerstian titration behavior for both hemes.

REFERENCES

Argade, P. V., Ching, Y. C., & Rousseau, D. L. (1986) *Biophys. J. 50*, 613–620.

Artzabanov, V. Yu, Konstantinov, A. A., & Sklachev, V. P. (1978) *FEBS Lett. 87*, 180–185.

Babcock, G. T. (1988) in *Biological Applications of Raman Spectroscopy* (Spiro, T. G., Ed.) Vol. III, pp 293–346, John Wiley and Sons, New York.

Babcock, G. T., Vickery, L. E., & Palmer, G. (1978) *J. Biol. Chem. 261*, 11524–11537.

Babcock, G. T., & Callahan, P. M. (1983) *Biochemistry 22*, 2314–2316.

Blair, D. F., Martin, C. T., Gelles, J., Wang, H., Brudvig, G. W., Stevens, J. H., & Chan, S. I. (1983) *Chem. Scr. 21*, 43–53.

Blair, D. F., Ellis, W. R., Wang, H., Gray, H. B., & Chan, S. I. (1986) *J. Biol. Chem. 261*, 11524–11537.

Brunori, M., Antonini, G., Malatesta, F., Sarti, P., & Wilson, M. T. (1988) *Adv. Inorg. Biochem. 1*, 93–153.

Carithers, R., & Palmer, G. (1981) in *Interactions Between Iron and Proteins in Oxygen and Electron Transport* (Ho, C., & Eaton, W. C., Eds.) Elsevier, New York.

Chan, S. I., & Li, P. M. (1990) *Biochemistry 29*, 2–12.

Ching, Y. E., Argade, P. V., & Rousseau, D. L. (1985) *Biochemistry 24*, 4938–4946.

Choi, S., & Spiro, T. (1983) *J. Am. Chem. Soc. 105*, 3683–3692.

Ellis, W. R., Wang, H., Blair, D. F., Gray, H. B., & Chan, S. I. (1986) *Biochemistry 25*, 161–167.

Goodman, G. (1984) *J. Biol. Chem. 259*, 15094–15099.

Harmon, P. A., Hendler, R. W., & Levin, I. W. (1993) *Anal. Biochem.* (submitted for publication).

Hartzell, C. R., & Beinert, H. (1976) *Biochim. Biophys. Acta 423*, 323–328.

Hendler, R. W., & Westerhoff, H. (1992) *Biophys. J. 63*, 1586–1604.

Hendler, R. W., Subba Reddy, K. V., Shrager, R. I., & Caughey, W. S. (1986) *Biophys. J. 49*, 717–729.

Hinkle, P., & Mitchell, P. (1970) *J. Bioenerg. 1*, 45–60.

Jones, M. G., Bickar, D., Wilson, M. T., Brunori, M., Colosimo, A., & Sarti, P. (1984) *Biochem. J. 220*, 57–66.

Kojima, N., & Palmer, G. (1983) *J. Biol. Chem. 258*, 14908–14913.

Leigh, J. S., Wilson, D. F., Owen, C. S., & King, T. E. (1974) *Arch. Biochem. Biophys. 160*, 476–486.

Martin, C. T., Scholes, C. P., & Chan, S. I. (1985) *J. Inorg. Biochem. 23*, 233–242.

Minnaert, K. (1965) *Biochim. Biophys. Acta 110*, 42–56.

Nicholls, P., & Peterson, L. C. (1974) *Biochim. Biophys. Acta 357*, 462–467.

Nicholls, P., & Wrigglesworth, J. M. (1989) *Ann. N.Y. Acad. Sci. 550*, 59–67.

Ogura, T., Hon-Nami, K., Oshima, T., Yoshikawa, S., & Kitagawa, T. (1983) *J. Am. Chem. Soc. 105*, 7781.

Ogura, T., Yoshikawa, S., & Kitagawa, T. (1985) *Biochemistry 24*, 7746–7752.

Palmer, G., Babcock, G. T., & Vickery, L. E. (1976) *Proc. Natl. Acad. Sci. U.S.A. 73*, 2206–2210.

Pardhasaradhi, K., Ludwig, B., & Hendler, R. W. (1991) *Biophys. J. 60*, 408–414.

Scholes, C. P., & Malmstrom, B. G. (1986) *FEBS Lett. 198*, 125–129.

Schrager, R. I., & Hendler, R. W. (1986) *Biophys. J. 49*, 687–691.

Steffens, G. C. M., & Buse, G. (1988) *EBEC Rep. 100*.

Vanneste, W. H., & Vanneste, M.-T. (1965) *Biochem. Biophys. Res. Commun. 19*, 182–186.

Wikström, M., Harmon, J. H., Ingledew, J., & Chance, B. (1976) *FEBS Lett. 65*, 259–277.

Wikström, M., Krab, K., & Saraste, M. (1981) *Cytochrome Oxidase: A Synthesis*, Academic Press, New York.

Wilson, D. F., & Leigh, J. S. (1974) *Ann. N.Y. Acad. Sci. 227*, 630–635.

Wilson, D. F., Lindsay, J. G., & Brucklehurst, E. S. (1972) *Biochim. Biophys. Acta 256*, 277–286.

Wilson, D. F., Erecinska, M., & Owen, C. S. (1976) *Arch. Biochem. Biophys. 175*, 160–173.

Wrigglesworth, J. M., Elsden, J., Chapman, A., Vander Water, N., & Grahm, M. F. (1988) *Biochim. Biophys. Acta 936*, 452–464.

Yoshikawa, S., Choc, M. G., O'Toole, M. C., & Caughey, W. S. (1977) *J. Biol. Chem. 252*, 5498–5508.